RSC Advances

PAPER

View Article Online
View Journal | View Issue

Cite this: *RSC Adv.*, 2018, **8**, 42415

Utilizing FBR to produce olefins from CO reduction using Fe–Mn nanoparticles on reduced graphene oxide catalysts and comparing the performance with SBR†

AL-Hassan Nasser, *[ab] Hamada EL-Naggar[a] and Ahmed Abdelmoneim*[a]

Mn was used as a promoter for Fe nanoparticles (NPs) loaded on reduced graphene oxide (rGO). The prepared catalysts were the unpromoted Fe/rGO catalysts along with two Mn promoted catalysts FeMn16 and FeMn29. These catalysts were used as Fischer–Tropsch catalysts in a Fixed Bed Reactor (FBR). The operating conditions of the reactor, namely temperature, pressure and space velocity, were varied to evaluate the catalyst performance and the olefin productivity. The olefins were produced in maximum yields of 34.5% and 31.3% with FeMn29 at 320 and 340 °C respectively. The ratio of light to heavy olefins was three times higher at 340 °C. The catalysts showed good stability up to 50 h of interrupted operation while varying the conditions at each interruption. The performance of the catalysts in the FBR was compared with a previous investigation carried out in an SBR under identical conditions with the same catalysts. The FBR was found to be more Mn tolerant than the SBR, giving very high conversion activity with high Mn concentrations (FeMn29). The FBR produced olefins in much higher yields than the SBR. The SBR was more selective to light olefins at low temperatures and high Mn loading levels, while the FBR produced light olefins at higher selectivities at high temperatures and high Mn concentrations.

Received 30th October 2018
Accepted 6th December 2018

DOI: 10.1039/c8ra09003c

rsc.li/rsc-advances

1 Introduction

Olefins always play a major part in the petrochemical industry as they occupy a large fraction of the petrochemical market as feedstocks for many important end products such as commercial plastics, engineering polymers, pharmaceuticals and synthetic fibers.[1,2] Ethylene alone is described as "the largest value petrochemical commodity produced globally".[3] Many methods are available for the production of olefins from fossil fuels, the most intensively used method worldwide is steam cracking which is also the most energy consuming.[1,2] Other methods include methanol to olefins (MTO), oxidative coupling of methane (OCM), catalytic dehydrogenation of light alkanes, and finally the Fischer–Tropsch synthesis (FTS).[1–5]

FTS technology is a promising route to olefins. It is carried out industrially in four main reactor types: multi-tubular fixed bed reactors (FBR), Slurry Bed Reactors (SBR), Circulating Fluidized Bed Reactors (CFB), and the Fixed Fluidized Bed Reactors (FFB).[2,6]

On the research scale most work is either carried out in FBRs[7–10] or in SBRs.[11–13] To our knowledge, publications concerned with the difference in performance between the two reactors at the same operating conditions while using the same catalytic systems are not that common. In a previous investigation[11] we studied the effect of operating conditions on the olefin productivity of Mn promoted Fe/rGO catalysts in SBR at HTFT conditions. We had the chance to repeat the same experiments with the same catalysts and at the same conditions but in a FBR.

Manganese is a well renowned promoter used with Fe catalysts in FTS production to enrich the olefin content, increase average chain length of the product and to enhance activity within certain concentration limits.[11,14,15] Mn on its own is not a FT catalyst, but when added at small concentration to other FT catalysts like Fe it can increase carburization reactions and limit hydrogenation of olefins. The reason for this is that Mn increases surface basicity of the Fe nanoparticles, this rise in alkalinity enhances CO dissociative adsorption whilst discouraging H_2 dissociative desorption. This deprives the catalyst surface from the hydrogen radicals essential for chain terminating hydrogenation reactions which in effect increases olefinity and heavy hydrocarbon selectivity. However at very high

[a]*Materials Science and Engineering Department, Egypt-Japan University of Science and Technology, New Borg El-Arab, Alexandria 21934, Egypt. E-mail: codecsubzero@gmail.com; ahmed.abdelmoneim@ejust.edu.eg*

[b]*Chemical Engineering Department, Faculty of Engineering, Alexandria University, Alexandria 11432, Egypt*

† Electronic supplementary information (ESI) available. See DOI: 10.1039/c8ra09003c

concentrations it tends to isolate the Fe core from the reactants and deactivates the catalysts severely.[11,14–17] In general there exists an optimum Mn concentration range for the production of the desired hydrocarbon fraction outside which productivity of this fraction falls either due to low catalyst activity or due to poor selectivity for this particular fraction or due to both reasons combined.

In our work rGO was also utilized as a novel support material for the Fe–Mn nanoparticles. rGO is a famous new material that is attracting more and more attention since its reintroduction in research in the last two decades. rGO mainly produced from the modified Hummers method[9,11,18–20] was introduced into many applications in the a variety of fields, however research concerning the use of rGO in FTS technology is not that intensive when compared with other fields of application.[8,9,11,21–30] The work by Cheng[8,25] tried to study the olefinity of FTS products from Mg and alkali metal promoted Fe/rGO catalysts. It is also important to mention that to our knowledge no published work investigated rGO supported catalysts in SBR except our previous investigation.[11] Finally this is the first research effort that is concerned with the comparison between SBR and FBR for the Fe–Mn/rGO system.

In a previous investigation,[11] we studied for the first time the effect of operating conditions on the olefin productivity of Mn promoted Fe/rGO catalysts in SBR at High Temperature Fisher Tropsch (HTFT) conditions. In this study, a Mn concentration of 16 mol Mn/100 mol Fe was found to give a good olefin yield of 19% with an olefin/paraffin (O/P) ratio of 0.77 at 2 MPa, 300 °C and 4.2 l g^{-1} h^{-1} using syngas with a 1 : 1 H_2 : CO ratio.

Inspired by that work, we had the chance to repeat the same experiments conducted in SBR with the same catalysts and at the same conditions but in a FBR to form a better judgment or comparison on the catalytic performance of the novel Fe–Mn/rGO catalysts for FTS in both reactor systems. In fact, this is the first research effort concerned with the comparison between SBR and FBR for the Fe–Mn/rGO system which may support the future feasibility analysis and economic aspects of FTS relying on using this new generation of catalyst systems.

In the first part of the investigation the results obtained from the FBR recent experiments are presented and discussed. The study is further enriched with a stability study and a comparison with similar work in literature. Finally the results from both systems are plotted side by side compared. The comparison was based on activity enhancement, control of undesired and side reactions like WGS and methane production, and finally olefin selectivity and production yields.

2 Materials and methods

2.1 Catalyst preparations

The catalysts used in this work, namely Fe, FeMn16 and FeMn29, are the same catalysts that were used in the SBR investigation and were prepared by the same methods described in the previous work.[11]

Briefly, graphite oxide (GtO) was prepared by the modified Hummer's method in which graphite (10 g) was oxidized in a strong oxidizing mixture comprising of sulfuric (500 ml) and nitric acid (160 ml) along with $KMnO_4$ (60 g). This was followed by ultrasonic exfoliation, washing with HCl and distilled water (DW), centrifuge separation and drying to obtain the final GtO flakes.

The GtO flakes were then ultrasonically dispersed in 200 ml DW to form a GO suspension. To this suspension a doping solution (50 ml) containing the adequate amount of the $Fe(NO_3)_3 \cdot 9H_2O$ precursor salt was added drop wise while stirring the GO suspension mechanically.

After further stirring and homogenization for 8 h the mixture was heated up to 80 °C then reduced chemically by adding 22 ml of 80% Hydrazine Hydrate (HH) drop wise to obtain the reduced graphene oxide flakes decorated with the Fe_2O_3 nanoparticles after refluxing the mixture at 80 °C for. The mixture was then filtered washed to neutral PH and dried. The obtained Fe/rGO powder was stored in an air tight container for further use.

Doping of the catalysts with Mn was executed by ultrasonic assisted impregnation. 1 g of the catalyst was impregnated with a suitable amount of $MnNO_3 \cdot 6H_2O$ dissolved in 20 ml ethanol. The slurry was steam dried over a beaker of boiling water then dried at 60 °C for 6 h. The powder collected was stored in a vial and labeled FeMny where *y* represents the molar ratio of Mn per 100 mol Fe.

2.2 Characterization

A full characterization of the catalysts along with an attempt to describe the morphology of the Fe–Mn nanoparticles can be found in the work published previously.[11]

2.3 FTS fixed bed reactor performance evaluation

The FBR system used in this work was slightly modified from its original design described elsewhere[9] to imitate the product collection system of the SBR unit used in our previous investigation[11] since it was more effective in collecting the liquid products as displayed in Fig. 1. Thus the large hot and cold traps were replaced by a single cold trap with a 65 ml capacity. Before starting the run, 0.5 g of the catalyst powder diluted by an equal mass of SiC were loaded in the 0.5″ reactor pipe. The catalyst was calcined in He atmosphere (50 ml min^{-1}) at 300 °C for 3 h, followed by reduction at 450 °C for 16 h in H_2 atmosphere (50 ml min^{-1}). Afterwards the cold trap was filled with 20 ml DW and 2 g *n*-octane then sealed and cooled to 3 °C. The reaction conditions of *T*, *P* and syngas (H_2 : CO = 1 : 1) flow rate were then adjusted and the run was operated for the desired time on stream with online analysis of the exit gas stream in GC/TCD system fitted with a 3 m Shincarbon Restek Column to measure the CO, CH_4 and CO_2 levels. The permanent gas composition was calculated using external standards for each of the three gases. After steady state conditions were reached the light hydrocarbon content (up to C_6) of the exit gas is measured in GC/FID system equipped with Rt-QPlot Restek capillary column (30 m, 0.32 mm ID, 10 μm film). The liquid product was analyzed for higher hydrocarbons using GCMS system (Shimadzu-GCMS QP2010) after separation in an Agilent DB-5 column (60 m, 0.25 mm ID, 0.25 μm film). The areas of the separated products were compared with methane as an external

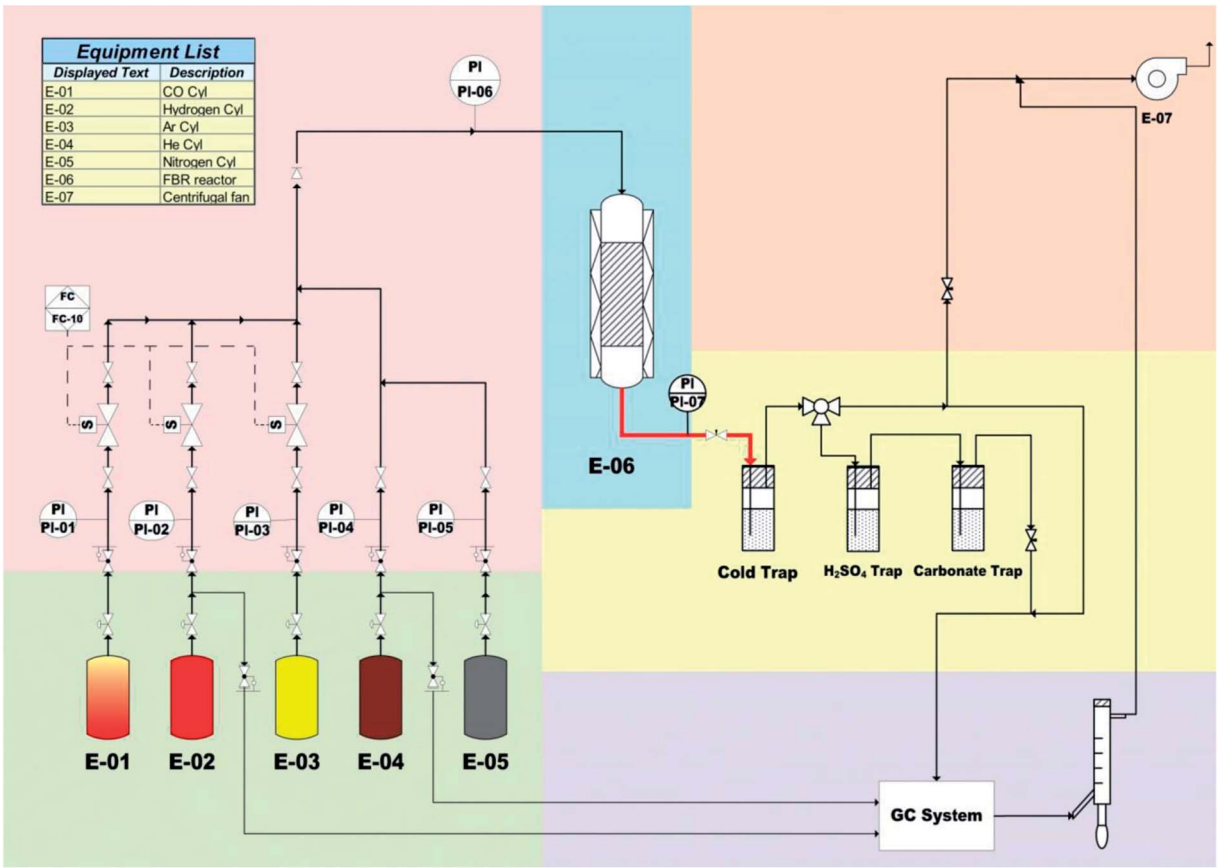

Fig. 1 Process flow diagram of the modified FBR unit.

standard in the gas FID, and with *n*-dodecane as an internal standard at 0.2 g in the GC/MS results. The olefin free chromatograms were produced after sulfuric acid absorption of the respective gas or liquid products to be able to calculate the olefin yield and selectivity.

In the GC/TCD analysis the injection ports were kept at 100 °C, the column was kept at 120 °C, and the TCD detector was heated to 150 °C, the while He gas carrier flow rates were 10 ml min^{-1}. The FID oven was kept at 50 °C for 5 min, and then the temperature was ramped up at 15° min^{-1} to 190. This temperature was held till the end of the GC test. The He carrier was supplied at a linear velocity of 40 cm s^{-1}. The samples were injected at a split ratio of 150. For the GC/MS liquid analysis the injection port was at 300 °C with a 26.3 split ratio, the column oven temperature was held at 40 °C for 5 min, the ramped up to 330 °C at 15°min, then held at this temperature for a further 10 min. The carrier gas was supplied at a linear velocity of 27.6 cm s^{-1}.

3 Results and discussion

3.1 FTS fixed bed reactor performance evaluation

3.1.1 Adjusting the operating conditions for high olefin yield. Variable sweep analysis of the FeMn catalyst system is a very effective method to find the best possible condition for olefin production. As a preliminary step the unpromoted catalyst Fe was tested at three temperature levels to get a sense of the catalyst performance limits. The three temperature levels are: 300, 320 and 340 °C while the pressure and GHSV were adjusted at: 2 MPa and 4.2 l g^{-1} h^{-1} respectively, as summarized in Fig. 2(a), and the complete details of the runs are given in Table S1.† A typical FTS performance is evident from the gradually rising conversion, WGSR and methane selectivity with temperature. The total olefin yield was generally low with Fe starting at a maximum of 7% at 300 °C to reach a minimum of 2% at 340 °C. It is expected that olefin productivity would fall at higher temperature which favor the saturation of the olefin π-bonds.

Fig. 2(b) illustrates that the same trend regarding WGSR and methane selectivity with FeMn16 at the same temperature levels. Also notable is the choking effect that Mn had on the methane selectivity staying below 20% at all times. The activity of the catalyst was significantly improved by Mn promotion, recording higher activity at all temperature levels starting with 60% at 300 °C and reaching a steady maximum of about 98% at 340 °C. Most importantly an olefin best condition can be spotted easily in the vicinity of 320 °C (maximum of 29% olefin yield). Which would be a good temperature level at which the performance of different catalysts can be compared.

The conditions of GHSV and pressure were also varied to complete the variable sweep study as summarized in Fig. 2(c and d). It is not farfetched to expect a weak effect of these variables on the catalyst performance since they already had no or negligible effects in the SBR system.[11] The levels for GHSV tested were 4.2, 6.2 and 8.2 l g^{-1} h^{-1}, with *T* and *P* kept at 320 °C

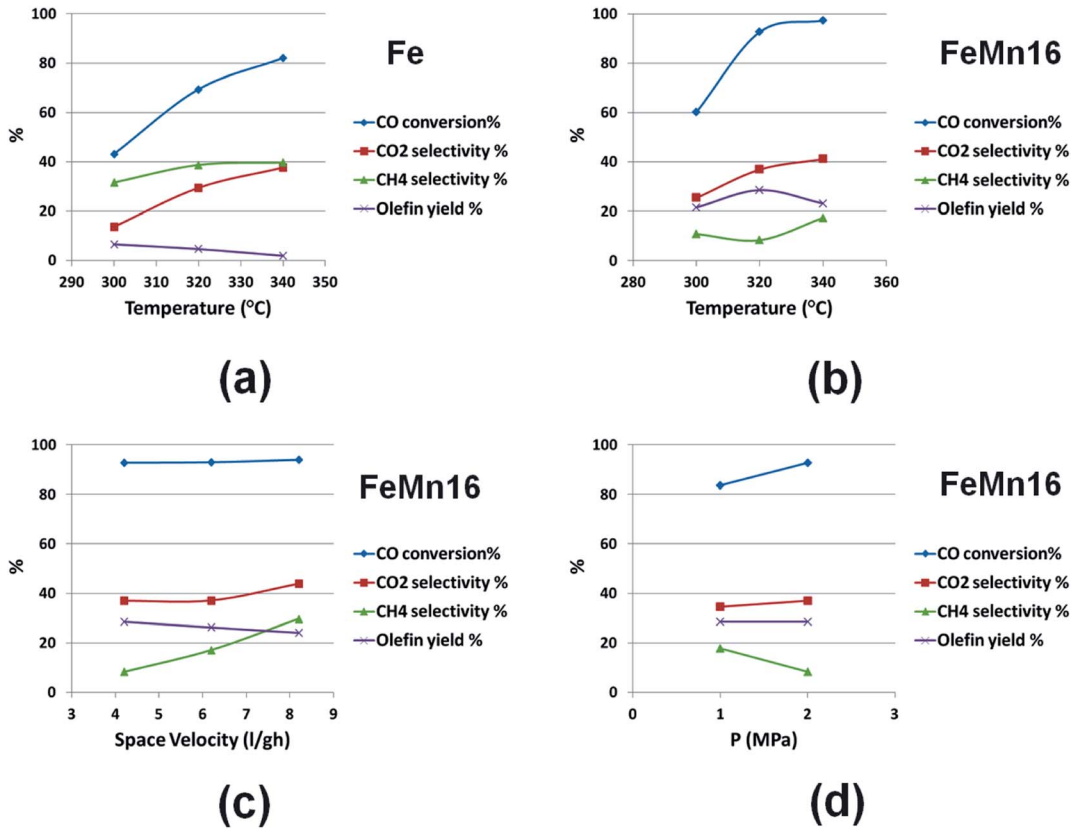

Fig. 2 Plots of CO conversion, CO_2 and CH_4 selectivities, and olefin yield for: (a) Fe and (b) FeMn16 at 4.2 l g^{-1} h^{-1}, 2 MPa and different temperatures, (c) FeMn16 at 320 °C, 2 MPa and different space velocities, and lastly (d) FeMn16 at 320 °C, 4.2 l g^{-1} h^{-1} and different pressures.

and 2 MPa respectively. Fig. 2(c) compares these results and shows that increasing the space velocity in this range did not affect the conversion or WGSR significantly and both stayed at 92% and 40% respectively. However there was a rise in CH_4 selectivity which leaped from 8.3% at 4.2 l g^{-1} h^{-1} to 23% at 8.2 l g^{-1} h^{-1}. This increase is normal due to the decrease in the average retention time of the reactants at the catalyst surface. This favors the production of shorter chain hydrocarbons in general and specifically increases the methane selectivity. This is further evidenced by the fall in the ASF factor which dropped from 0.77 at 4.2 l g^{-1} h^{-1} to 0.58 at 8.2 l g^{-1} h^{-1} as detailed in Table S2.†

The effect of the rising space velocity from 4.2 to 8.2 l g^{-1} h^{-1} on olefinity was slightly negative causing a decrease in olefin yield from 28.56 to 24.16%. It is worth noting however that the quality of the olefin stream showed a steady increase in light olefins C_{2-4} and a simultaneous decrease in heavy olefins C_{5-9} as the GHSV increased to 8.4 l g^{-1} h^{-1} as clarified. Thus changing the GHSV can prove to be a useful tool in changing the olefin orientation of the catalyst towards lighter or heavier olefins as dictated by the market dynamics. The same trend was also observed with the paraffins, where the C_{9+} selectivity plummeted from 21% at 4.2 l g^{-1} h^{-1} to 7% only at 8.2 l g^{-1} h^{-1}, which is a threefold decrease as listed in Table S2.† Finally, there was an overall decrease in isoparaffin content with rising space velocity since probabilistically longer chains produce more isomers, and a condition favoring the formation of shorter chain hydrocarbons will definitely cause a decrease in the isomer content of the product.

The final variable tested was the pressure which was varied by one level only to test the performance at 1 MPa as displayed in Fig. 2(d). The effect of pressure was negligible towards WGSR and the total olefin yield. The CO conversion increased at higher pressures, while the methane selectivity was adversely affected. Higher pressures provide a higher reactant concentration at the catalyst surface and thus are expected to favor higher conversions and the production of longer chain hydrocarbons, which would explain the fall in methane selectivity with pressure. This is further reinforced by the details in Table S3† which shows an increase in α from 0.63 at 1 MPa to 0.77 at 2 MPa, accompanied by a remarkable rise in the C_{9+} hydrocarbons from 8.5 to 21.3% and isoparaffins from 10.6 to 24.6%. Interestingly the total selectivity of saturated hydrocarbons (paraffins and isoparaffins) as well as olefins stayed almost constant at 50–50% but the quality of olefins changed dramatically with pressure, tending towards higher olefins C_{5-9} as the pressure increased, while the total olefin yield stayed constant with pressure at about 28%.

After looking at the variable sweep study, it is reasonable to conclude that for the highest possible olefin yield it is advised to operate at a moderate temperature in the 300–320 °C range and at low flow rates 4.2 l g^{-1} h^{-1} to avoid excessive methane production, while the pressure can be varied according to the required olefin fraction quality. However it is important to

recognize that the conversion declined at low pressures without a notable quantitative improvement in olefin yield. Hence to further study the effect of Mn promoter level the pressure and space velocity will be fixed at 2 MPa and 4.2 l g^{-1} h^{-1} respectively, while the temperature will be varied from 300 to 340 °C to get a deeper assessment of the promoter effect with temperature.

3.1.2 Effect of Mn concentration on olefin yield. Three levels of Mn concentration were used in this part of the study, the unpromoted Fe catalyst and two Mn promoted catalysts FeMn16 and FeMn29. They were all tested at 2 MPa, 4.2 l g^{-1} h^{-1} and at three temperature levels: 300, 320, and 340 °C. The results are plotted in Fig. 3(a–d) and the details are compared in Table S1.†

Mn enhanced the catalyst activity at the 16/100 mol Fe ratio, beyond which the data clearly shows the deactivation caused by Mn at 29 mol/100 mol Fe; this deactivation effect is found to be less severe as the temperature is raised from 300 to 340° as clarified in Fig. 3(a). At the same time, the WGSR activity in Fig. 3(b) followed the same suite as the conversion activity mirroring the initial enhancement in CO_2 selectivity at 16/100 mol Fe followed by a mild fall at 29/100 mol Fe. As was discussed before in the SBR investigation,[11] Mn on its own is not a Fischer–Tropsch catalyst, it is thus a chemical promoter which can only improve the performance of FTS catalysts like Fe. At very high concentrations, and with its tendency to form a Mn rich outer shell encapsulating the Fe rich catalyst core,[7,11,15,17] it was demonstrated previously and in detail how this nature would have a negative impairment on the FTS catalyst activity and WGSR.

Furthermore, Mn had a similar restraining effect on the methane selectivity as seen in Fig. 3(c) holding it down at all conditions to below 25%. The highest selectivity at 340 °C with FeMn29 was 24%, as opposed to the unpromoted Fe catalyst which recorded a minimum methane selectivity of 32% at 300 °C. The ability of Mn to hold down the CH_4 content in the product is less pronounced beyond 320 °C where the very high temperatures dominate the reaction kinetics forcing more methane production. Anyways, this methane choking effect proves very valuable since methane in many FTS technologies is an undesired low calorific value product when compared with heavier hydrocarbon fractions. In other cases the main feedstock of the syngas is originally natural gas converted through steam or oxygen cracking into CO and H_2, which renders high methane selectivity FTS systems completely useless and undesirable.

Olefin productivity as illustrated in Fig. 3(d) is vastly improved by Mn doping. The olefin yield soared to 28.6% with FeMn16, and to 34.5% with FeMn29 at 320 °C as well. The best condition for high olefin productivity can be chosen at 320 °C with FeMn29 which gives a 1 : 1 ratio between light (28.01%) and heavy olefin (28.13%) selectivities. At 340 °C FeMn29 also gave a very similar olefin yield (31.5%) but with an olefin product richer in light olefins than at 320 °C, with a light (40%)

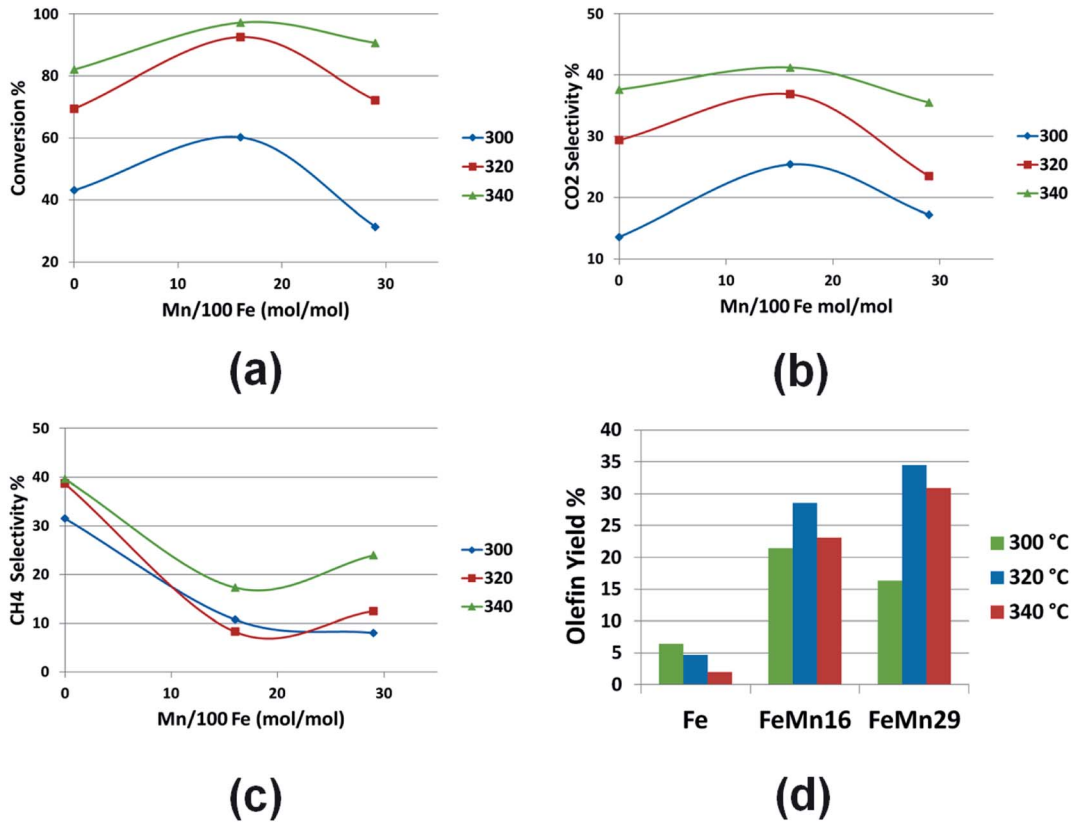

Fig. 3 Plots of (a) CO conversion, (b) CO_2 and (c) CH_4 selectivities, and (d) olefin yields for the three catalysts Fe, FeMn16 and FeMn29 at different temperatures.

to heavy olefin (14%) selectivity ratio of about 3 : 1 (threefold increase in light olefins).

In a previous detailed discussion of the effect of Mn on the reaction mechanism,[11,15–17] it was stated that the increased site basicity induced by Mn promotion enhances CO dissociative adsorption whilst discouraging H_2 dissociative adsorption. It was then deduced that this intrinsic behavior of the active site will directly retard hydrogenation reactions (saturation of olefinic π-bonds) and support the chain growth by providing more carbonic radicals to be assembled in the growing chains while starving the active sites of hydrogen radicals. These radicals are mainly responsible for chain termination and double bond saturation reactions. Such a kinetic model dictates that Mn promotion will lead to a reduction in methane, along with a surge in olefinity and a rise in the average molecular weight of the product.

This effect when unobstructed by the high temperatures produces products richer in heavy olefins as well as light olefins and isoparaffins. However the excessive rise in temperature especially above 320 °C overcomes the Mn promoting effect and the catalysts tend to slightly imitate the behavior of an unpromoted catalyst. That is the reason behind the increase in methane selectivity and shift of the product distribution out into the light ends region where light olefins dominate the scene and heavy paraffins and isoparaffins diminish again. A look at Fig. 3(d) and a thorough look at Table S1† will assert such predictions.

3.1.3 Comparison with other work in literature. The most notable work among all the literature published in the past five years concerning the production of olefin from promoted Fe/rGO catalysts is detailed in the two publications by Y. Cheng and coworkers.[8,25] The reaction conditions are very similar to ours, operating at 20 bars, 613 K or 340 °C, with a 1 : 1 syngas feed. The feed rate however was varied in each run to keep the conversion almost constant within the 59–64% range. Another important similarity is in the catalyst preparation methods, where we originally adopted the hydrothermal method for the decoration of rGO with Fe NPs from their work as well.

The major difference is in the constituents of the catalytic systems, in their first publication they tested potassium as a promoter to increase olefinity.[25] In 2017 they followed up by studying the effect of Mg among other GII elements as olefinity promoters, then they finally tested a ternary mixture catalyst comprising of Fe–K–Mg to optimize it for the production of olefins. On the other hand our system clearly is a binary component catalyst consisting only of Fe and Mn. Another minor difference is in the calculation method; where we calculate the total yield% as the ratio of the total olefins produced to the total CO feed, they calculate the olefin FT yield (FTY_{ole} μmol HC g_{Fe}^{-1} s^{-1}) which excludes CO_2 and unreacted CO. We recalculated the yield ratios in agreement with our method to be able to make a fair comparison as shown in Table 1.

Firstly, it is clear from Table 1 that Mn proved to be better in controlling the WGSR activity, where our maximum CO_2 selectivity was 37%, the selectivities recorded in the other studies start at 40%. Secondly, K is a well known FTS alkali metal promoter; at low concentrations it intensively increases the selectivity towards light olefins; previous work by Yi thus concentrated only on the C_{2-4} olefin fraction. This fraction was produced at higher selectivity in their work but at comparable yields to our results. So if the comparison is to be based on light olefins yield alone, it is clear from the results that both systems have a matching productivity.

An added advantage to the Fe–Mn system is in the significant heavy olefins yield, where the other system has obviously no data concerning the heavy olefin production, the Fe–Mn system can produce olefins with selectivities ranging from 14 to 28% and yields between 8 and 17%. And in total the Fe–Mn system was superior in producing olefins to the Fe–Mg–K system in all three recommended combinations, where the total olefin yield ranged between 29 and 35% for the Fe–Mn system, the maximum yield recorded with the other system was 23%.

This comparison thus proves the success of Fe–Mn in producing olefins at matching if not larger capacities than Fe–Mg–K system. Furthermore, it opens the question about the margin of improvement achievable if K is used in a ternary mixture with Fe and Mn, however this question may be answered only through further research.

3.1.4 Stability of the catalysts. The activity of FeMn16 and FeMn29 was monitored for 50 h, in this test the catalysts were exposed to different operating conditions with interrupted reactor operation to allow for product collection and temperature adjustment for the new stage. The results plotted in Fig. 4, for both catalysts show a good performance with acceptable stability. In Fig. 4(a) the catalyst returned to the same activity at 340 °C after operating at 320 °C showing no signs of

Table 1 Comparison of the olefin selectivity and yield with other work in literature

Catalyst	CO_2 sel.%	C = 2–4 sel.[a]%	C = 5–9 sel.[a]%	C = 2–4 yield%	Olefin yield
FeMn16 320 °C	37	20	25	13	29
FeMn29 320 °C	23	28	28	18	35
FeMn29 340 °C	36	40	14	23	31
FeK2 340 °C (ref. 25)	49–52	68	N/A	21[b]	21[b]
FeMg28 340 °C (ref. 8)	40.7	33	N/A	13[b]	13[b]
FeMgK2 340 °C (ref. 8)	40.8	65	N/A	23[b]	23[b]

[a] The selectivity is calculated per total hydrocarbons produced. [b] The total olefin yield is corrected for the CO_2 and the unreacted CO. $\text{Olefin yield}_{\text{Total}}\% = \frac{FTY_{ole} \times (100 - CO_2\ \text{sel.}\%) \times \text{CO conv}\%}{FTY \times 100}$.

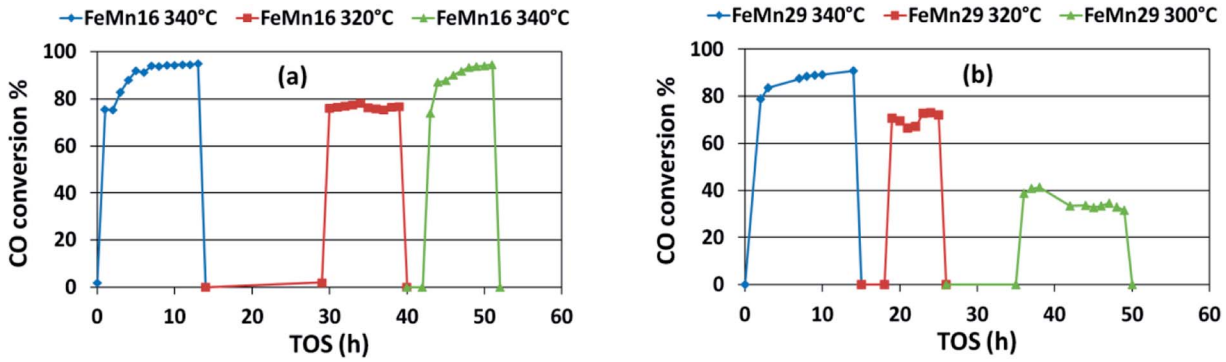

Fig. 4 Stability of (a) FeMn16 and (b) FeMn29 during 50 h operation at varying temperatures.

deactivation. With FeMn29 the temperature was decreased in each stage starting at 340 °C and ending at 300 °C. Again the catalyst displayed a typical decrease in activity as the temperature decreased but without showing any strong deactivation tendencies.

3.2 Comparison between SBR and FBR

Repeating the experiments with the same FeMn series on both the SBR[11] and the FBR systems allows drawing overall notes on the different performances of each reactor. The Fig. 5–8(a–c) compare the main performance parameters of the two reactors at 300 and 340 °C for the three catalysts (Fe, FeMn16 and FeMn29) and in the 280–340 °C for FeMn16. The comparison focuses on conversion, olefin selectivity for the C_{2-4} and C_{5-9} fractions, and finally the total olefin yield.

Fig. 5(a) shows that the catalyst activity is slightly better in the SBR than FBR with the unpromoted Fe catalyst at 300 °C. While the difference in conversion is very small with the two Mn promoted catalysts. On the other hand, when the temperature is raised from 320 to 340 °C as displayed in Fig. 5(b), the activity of the unpromoted Fe catalysts is the same in both reactors, as opposed to the Mn promoted catalysts which gave higher activities in the FBR than in the SBR at 340 °C. The same behavior holds with FeMn16 in the 280–340 °C plotted in Fig. 5(c) with FBR activity surpassing that in the SBR at higher temperatures.

It could be argued that the SBR system is a three phase system in which the reactants travel to the catalyst surface from the gas phase first through the oil phase by absorption followed by diffusion and adsorption on the catalyst surface; absorption in the SBR is an extra stage not required in the FBR. Furthermore absorption being exothermic becomes more difficult as temperatures rises, and so there is a balance between two opposing forces in the SBR that change relatively with temperature. On one hand heat increases the intrinsic activity of the active sites; on the other hand raising the temperature decreases the average residence time of the reactants in the oil, and so overall the CO conversion is not expected to rise to the same extent in the SBR as in the FBR at high temperatures. Also the gap in conversion between the two reactors increases with Mn loading % as clarified in Fig. 5(b). As a general conclusion the SBR is more suited for low temperature operation with moderate Mn loading levels, while FBR gives better activities at higher temperatures and is more Mn tolerant than SBR.

To study the effect of the reactor type on the olefin productivity, the discussion will be divided into three parts, one dealing with the effect on light C_{2-4} olefins selectivity as plotted in Fig. 6(a–c), the second concerning heavier olefins selectivity in the C_{5-9} range displayed in Fig. 7(a–c), and the last part looks at the overall total olefin yield as illustrated in Fig. 8(a–c).

By comparing Fig. 6(a and b) it is clear that at low temperatures (300 °C), the SBR produces light olefins at higher selectivities than FBR. The same observation holds with FeMn16 in the 280–340 °C range in Fig. 6(c). Unpromoted Fe catalyst gives nearly the same selectivity regardless of temperature. On the other hand, the behavior at high temperatures beyond 300 °C is not simple, with a reverse point at FeMn16 in Fig. 6(b) below which SBR is more selective to light olefins and above which FBR produces more light olefins. The same behavior appears

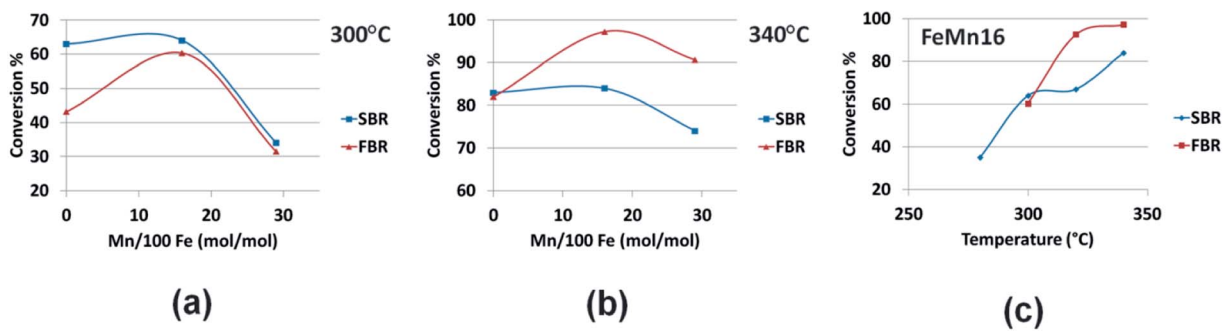

Fig. 5 Comparing SBR and FBR conversions for the FeMn series at (a) 300 °C, (b) 340 °C and for (c) FeMn16 in 280–340 °C range.

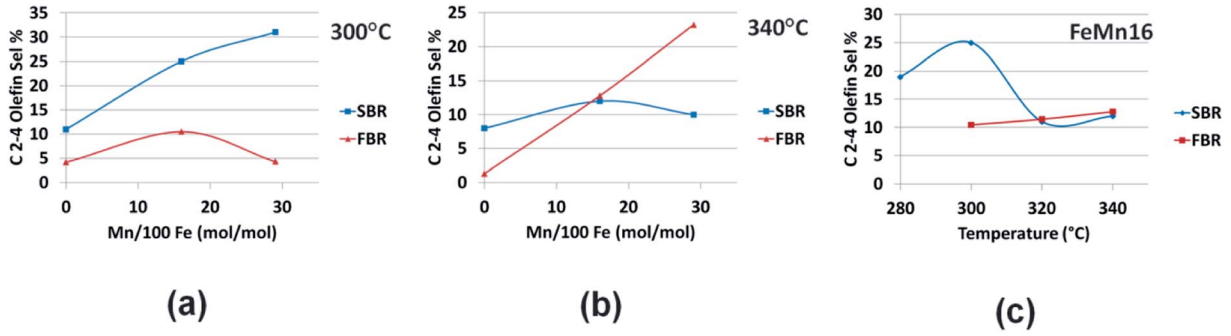

Fig. 6 Comparing SBR and FBR C_{2-4} olefin selectivities for the FeMn series at (a) 300 °C, (b) 340 °C and for (c) FeMn16 in 280–340 °C range.

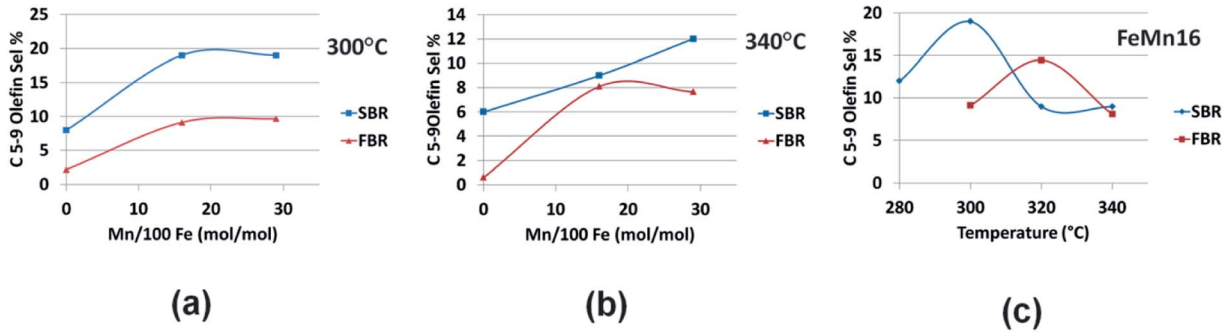

Fig. 7 Comparing SBR and FBR C_{5-9} olefin selectivities for the FeMn series at (a) 300 °C, (b) 340 °C and for (c) FeMn16 in 280–340 °C range.

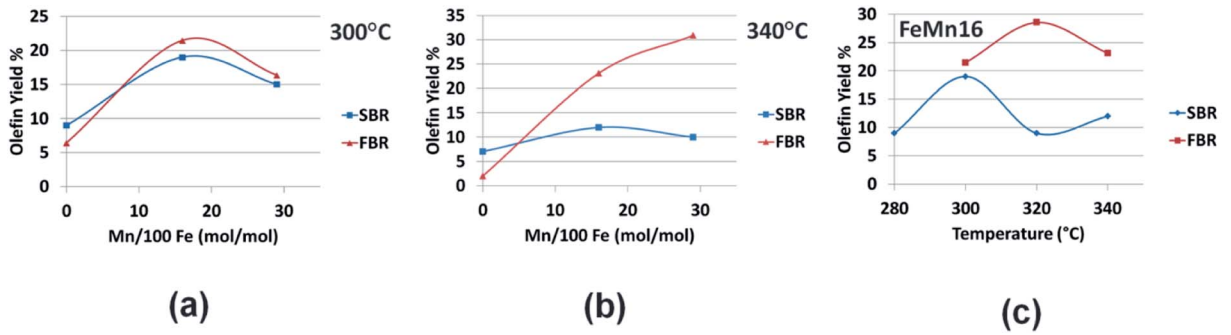

Fig. 8 Comparing SBR and FBR olefin yields for the FeMn series at (a) 300 °C, (b) 340 °C and for (c) FeMn16 in 280–340 °C range.

with FeMn16 in the 280–340 °C in Fig. 6(c), with SBR giving off more light olefins below 320 °C, and both reactors give the same selectivity for light olefins at higher 320 °C and beyond.

SBR is more selective for the C_{5-9} olefins at all concentration and temperatures except for one case with FeMn16 at 320 °C in which FBR produces more heavy olefins as demonstrated in Fig. 7(a–c). Of course, the selectivities are boosted at lower temperatures due to the increased chain growth probability and reactant residence time. In general we can expect that SBR is more selective to olefins especially heavy fractions at low temperatures and high Mn promotion %, while FBR is more selective to light olefins at high temperatures and Mn concentrations.

Although selectivity gives some measure of the product quality, the true sense of the FTS productivity towards a certain fraction is better grasped through the yield parameter as illustrated in Fig. 8(a–c). At low temperatures the olefin yields, plotted in Fig. 8(a), show very slight variation in value between FBR and SBR at different Mn loading levels. As the temperature is increased to 340 °C FBR proves to be more effective is producing olefins than SBR only when the catalysts are promoted with Mn. The olefin yield rises significantly with Mn loading reaching a maximum of about 31% with FeMn29. The same trend is true with FeMn16 in the 280–340 °C range with a local maximum of 29% at 320 °C.

4 Conclusion

Mn acted effectively as a promoter for Fe by enhancing activity and WGSR at Mn loading 16/100 mol Fe, while restraining

methane selectivity. Further rise in Mn concentration (29/100 mol Fe) caused slight deactivation of the catalyst and WGSR, with a very small rise in methane selectivity. Mn also pushes the selectivity to heavier hydrocarbons so that at moderate temperatures up to 320 °C there is a rise in heavy olefins, heavy hydrocarbons and isoparaffins. But at higher temperatures the effect of temperature overcomes that of Mn and the average molecular weight of the product decreases again accompanied by a fall in isoparaffins and heavies and a surge in light olefins and methane.

Olefin productivity was intensely improved by Mn promotion in the FBR system recording yields as high as 34.5% and 31.3% when using FeMn29 at 320 and 340 °C respectively, with a threefold increase in the light to heavy olefin ratio as temperature rises from 320 °C to 340 °C.

An optimum condition for producing light olefins would be at 2 MPa, 4.2 l g^{-1} h^{-1}, and 340 °C using FeMn29. While the same catalyst can be used at the same pressure and GHSV but at 320 °C if the aim is at heavier olefins. And both catalysts FeMn6 and FeMn29 gave good stability results for 50 h with interrupted operation showing no signs of deactivation.

The SBR gives better activity at low temperatures with moderate Mn loading levels, while FBR gives better activities at higher temperatures. On the other hand, FBR had a higher tolerance for Mn than SBR; operating at higher activities than SBR at high Mn loading levels.

Generally speaking, with Mn promoted Fe catalysts, FBR produces olefins at higher yields than SBR. In the SBR, the C_{5-9} olefin selectivity is higher than FBR at low temperatures and high Mn promotion %, while FBR is more selective to light olefins at high temperatures and Mn concentrations.

Conflicts of interest

There are no conflicts of interest to declare.

Acknowledgements

This research was conducted as a part of Research Project (ID 4543) supported by the Science and Technology Development Fund (STDF) in Egypt. The first author is deeply grateful to the Mission Sector-MOHE for providing a PhD degree scholarship fund, the Materials Science and Engineering Department at E-JUST, and the Japan International Cooperation Agency (JICA) for support of this work.

References

1 T. Ren, M. Patel and K. Blok, *Energy*, 2006, **31**, 425–451.
2 I. Amghizar, L. A. Vandewalle, K. M. Van Geem and G. B. Marin, *Engineering*, 2017, **3**, 171–178.
3 A. Boulamanti and J. A. Moya, *Renewable Sustainable Energy Rev.*, 2017, **68**, 1205–1212.
4 Q. Zhang, S. Hu and D. Chen, *J. Cleaner Prod.*, 2017, **165**, 1351–1360.
5 D. Gao, X. Qiu, Y. Zhang and P. Liu, *Comput. Chem. Eng.*, 2018, **109**, 112–118.
6 L. Bai, H. Xiang, Y. Li, Y. Han and B. Zhong, *Fuel*, 2002, **81**, 1577–1581.
7 T. Li, Y. Yang, C. Zhang, X. An, H. Wan, Z. Tao, H. Xiang, Y. Li, F. Yi and B. Xu, *Fuel*, 2007, **86**, 921–928.
8 Y. Cheng, J. Lin, T. Wu, H. Wang, S. Xie, Y. Pei, S. Yan, M. Qiao and B. Zong, *Appl. Catal., B*, 2017, **204**, 475–485.
9 A. H. M. Nasser, H. M. Elbery, H. N. Anwar, I. K. Basha, H. A. Elnaggar, K. Nakamura and A. A. El-Moneim, *Key Eng. Mater.*, 2017, **735**, 143–147.
10 D. B. Bukur, D. Mukesh and S. A. Patel, *Ind. Eng. Chem. Res.*, 1990, **29**, 194–204.
11 A.-H. Nasser, L. Guo, H. ELnaggar, Y. Wang, X. Guo, A. AbdelMoneim and N. Tsubaki, *RSC Adv.*, 2018, **8**, 14854–14863.
12 C. H. Zhang, H. J. Wan, Y. Yang, H. W. Xiang and Y. W. Li, *Catal. Commun.*, 2006, **7**, 733–738.
13 V. a. De La Peña O'Shea, M. C. Alvarez-Galvan, J. M. Campos-Martin and J. L. G. Fierro, *Catal. Lett.*, 2005, **100**, 105–110.
14 C. Wang, Q. Wang, X. Sun and L. Xu, *Catal. Lett.*, 2005, **105**, 93–101.
15 Z. Yang, X. Pan, J. Wang and X. Bao, *Catal. Today*, 2012, **186**, 121–127.
16 Q. Chen, G. Liu, S. Ding, M. Chanmiya Sheikh, D. Long, Y. Yoneyama and N. Tsubaki, *Chem. Eng. J.*, 2018, **334**, 714–724.
17 J.-D. Xu, K.-T. Zhu, X.-F. Weng, W.-Z. Weng, C.-J. Huang and H.-L. Wan, *Catal. Today*, 2013, **215**, 86–94.
18 W. S. Hummers and R. E. Offeman, *J. Am. Chem. Soc.*, 1958, **80**, 1339.
19 D. C. Marcano, D. V. Kosynkin, J. M. Berlin, A. Sinitskii, Z. Sun, A. Slesarev, L. B. Alemany, W. Lu and J. M. Tour, *ACS Nano*, 2010, **4**, 4806–4814.
20 M. Hirata, T. Gotou, S. Horiuchi, M. Fujiwara and M. Ohba, *Carbon*, 2004, **42**, 2929–2937.
21 H. Zhao, Q. Zhu, Y. Gao, P. Zhai and D. Ma, *Appl. Catal., A*, 2013, **456**, 233–239.
22 S. O. Moussa, L. S. Panchakarla, M. Q. Ho and M. S. El-Shall, *ACS Catal.*, 2014, **4**, 535–545.
23 B. Sun, Z. Jiang, D. Fang, K. Xu, Y. Pei, S. Yan, M. Qiao, K. Fan and B. Zong, *ChemCatChem*, 2013, **5**, 714–719.
24 X. Chen, D. Deng, X. Pan, Y. Hu and X. Bao, *Chem. Commun.*, 2015, **51**, 217–220.
25 Y. Cheng, J. Lin, K. Xu, H. Wang, X. Yao, Y. Pei, S. Yan, M. Qiao and B. Zong, *ACS Catal.*, 2016, **6**, 389–399.
26 F. Jiang, B. Liu, W. Li, M. Zhang, Z. Li and X. Liu, *Catal. Sci. Technol.*, 2017, **7**, 4609–4621.
27 S. Taghavi, A. Asghari and A. Tavasoli, *Chem. Eng. Res. Des.*, 2017, **119**, 198–208.
28 S. Karimi, A. Tavasoli, Y. Mortazavi and A. Karimi, *Appl. Catal., A*, 2015, **499**, 188–196.
29 Z. Hajjar, M. Doroudian Rad and S. Soltanali, *Res. Chem. Intermed.*, 2017, **43**, 1341–1353.
30 J. Huang, W. Qian, H. Ma, H. Zhang and W. Ying, *RSC Adv.*, 2017, **7**, 33441–33449.